Received 19 January 2023; revised 7 February 2023; accepted 16 February 2023. Date of publication 22 February 2023; date of current version 6 March 2023.

Digital Object Identifier 10.1109/OJAP.2023.3247173

The 3D-Printed Non-Radiating Edge Gap-Coupled Curved Patch Antenna

GIACOMO MUNTONI, GIOVANNI A. CASULA (Senior Member, IEEE), AND GIORGIO MONTISCI (Senior Member, IEEE)

Dipartimento di Ingegneria Elettrica ed Elettronica, Università degli Studi di Cagliari, 09123 Cagliari, Italy

CORRESPONDING AUTHOR: G. MONTISCI (e-mail: giorgio.montisci@unica.it)

ABSTRACT The use of parasitic resonant patches is a widespread technique to improve the bandwidth of microstrip patch antennas. Exploiting the free form-factor allowed by 3D-printing manufacturing technology, we present here a novel curved patch antenna layout, based on the non-radiating edge gap-coupled patch configuration. The proposed antenna is composed of a central curved patch, fed by a coaxial probe, and two gap-coupled parasitic side curved patches. This solution features a percentage impedance bandwidth of 16.3% using symmetrical parasitic side patches and 31.5% using asymmetrical side patches. A significant improvement of the bandwidth in comparison with both the standard non-radiating edge gap-coupled microstrip antenna (6.1% bandwidth) and the standard curved patch antenna (9% bandwidth) is achieved. Design and optimization of the proposed configuration are performed using the commercial software CST Studio Suite at the center frequency of 2.45 GHz. Prototypes of the symmetrical curved non-radiating edge gap-coupled patch antenna have been manufactured for the experimental verification, using a curved 3D-printed polylactic acid (PLA) substrate, fabricated with the commercial 3D printer PRUSA MK3S+, and a 50μm-thick adhesive aluminum tape for the metallization. Measured results show a very good agreement with simulations.

INDEX TERMS Curved patch, bandwidth enhancement, microstrip antennas, 3D printed antennas.

I. INTRODUCTION

FAST prototyping techniques for antennas and microwave devices fabrication, such as 3D-printing, are gaining increasing attention within the scientific community, thanks to their less time-consuming and low-cost approach [1], [2]. Aside from these glaring benefits, one of the primary advantages consists in the free-form factor, which bestows on the designer the ability to shape the dielectric component of radio frequency structures in an unusual but convenient fashion, exploiting the third dimension to obtain better overall performance [3], [4]. It is the case of the 3D-printed curved patch antennas recently proposed in [5] and [6], which take advantage of the cylindrical shape of the dielectric substrate to broaden the bandwidth, and at the same time, to increase the efficiency and reduce the projected planar resonant length of the patch antenna.

As shown in [7], the bandwidth can be further increased relying on well-known techniques, such as the stacked configuration or the inclusion of an incased air-gap inside the substrate.

In this paper, we investigate the effects of yet another designing technique to further boost the bandwidth of the conventional flat patch antenna, based once again on the curved layout, obtainable through 3D-printing, but also on the non-radiating edge gap-coupled microstrip antenna (NEGCOMA) configuration. In the NEGCOMA, two additional parasitic resonators are placed next to the central patch, along the resonant length, separated by a small gap [8]. The length of the side resonators is slightly different from the main one, providing the broader bandwidth behavior. The parasitic patches can be identical, and as such, the antenna is defined as symmetrical NEGCOMA, or differ in size, resulting in an asymmetrical NEGCOMA. In comparison, the latter configuration, thanks to the size diversity, has a larger bandwidth, but it is flawed by a non-optimal radiation pattern throughout the entire operating band, due to the shift of the maximum from the broadside direction [8].

In general, the addition of multiple side resonators is widely used, with plenty of examples in the scientific literature for single antennas. They include 5G applications [9],

TABLE 1. State-of-the-art comparison. The radiating element dimension is normalized to the free space wavelength λ_0 at the center frequency.

Reference	Center frequency (GHz)	Bandwidth (%)	Method for improving bandwidth	Radiating element planar dimension (Length × Width)	Gain (dBi)	(ε_r) Substrate	Efficiency @ center frequency (%)
[5]	2.45	9	Curved patch	0.18 λ_0 × 0.38 λ_0	6.28 @ 2.45 GHz	2.55	86
[6]	2.15	13.3	Curved patch with stacked configuration	0.21 λ_0 × 0.43 λ_0	6 – 7	2.3	96
[8] Symmetrical NEGCOMA	3.14	6.1	NEGCOMA	0.3 λ_0 × 1.27 λ_0	NA	2.55	NA
[8] Asymmetrical NEGCOMA	3.11	7.2	NEGCOMA	0.3 λ_0 × 1.25 λ_0	NA	2.55	NA
[9]	28	20.2	Parasitic element and slots	0.47 λ_0 × 0.30 λ_0	3.5 – 6.9	4.4	82
[10]	36.5	13.1	NEGCOMA	0.28 λ_0× 1.62 λ_0	4.5 – 5.1	3	< 79
[11]	28	37.5	Stacked configuration/air-gaps, and coupled patches	0.78 λ_0 × 0.88 λ_0	6 – 10.7	3.6	88
[12] E-coupled MIMO	5.4	14.8	E-coupled parasitic patches (NEGCOMA)	0.33 λ_0× 0.82 λ_0	5.2 – 6.8	2.2	NA
[12] H-coupled MIMO	5.4	14.8	H-coupled parasitic patches	0.51 λ_0 × 0.49 λ_0	3.8 – 7.0	2.2	NA
[13]	3.5	8.3	Substrate/air-gap/substrate and coupled patches	0.40 λ_0× 0.38 λ_0	5 – 6.83	2.55	NA
[14]	L/S-band (1.75/1.85/ 1.96/2.14/2.6)	Multi-band	Two-patch configuration with coupled element	0.18 λ_0– 0.27 λ_0 × 0.85 λ_0– 1.25 λ_0	-1.7 – 4.8	4.4	14 – 44
This work (symmetrical)	2.45	16.3	NEGCOMA and curved layout	0.22 λ_0× 0.55 λ_0	6.5 – 7.3	2.55	95
This work (asymmetrical)	2.45	31.5	NEGCOMA and curved layout	0.23 λ_0× 0.55 λ_0	6.2 – 7.5	2.55	92

[10], Antenna-in-Package (AiP) solutions [11], MIMO antenna systems [12], [13], and automotive applications [14]. All these prototypes rely on subtractive manufacturing technology, such as the metallized substrate etching process, as there is no evidence of 3D-printed antennas, least of all curved layouts adopting this solution.

As apparent from the comparison in Table 1, the antenna proposed in this work takes advantage of the combined effect of both the NEGCOMA configuration and the curved layout, enabled by the 3D-printing manufacturing technology. This solution features an improved bandwidth with respect to both its planar counterpart [8], the standard curved patch [5], and the curved patch with stacked configuration [6]. Moreover, it allows an outstanding reduction of the planar resonant length, while keeping a reasonably small width of the radiating element in comparison with similar configurations [8], [10], [12]. The latter feature makes the proposed curved NEGCOMA also suitable for the implementation of planar arrays.

The symmetrical 3D-printed curved NEGCOMA is characterized by a total fractional impedance bandwidth of 16.3%, with an overall increase of more than 10% over the planar NEGCOMA, an efficiency of 95.6%, and a gain of about 7.3 dBi at 2.45 GHz. A thorough analysis of an asymmetrical NEGCOMA configuration is also reported in the interest of completeness, reaching a bandwidth of more than 30%, but at the expense of a deterioration of the radiation pattern. The same deterioration of the radiation characteristics can be observed in the flat asymmetrical NEGCOMA presented in [8].

This paper is organized as follows: Section II is dedicated to the design and simulation of the 3D-printed curved NEGCOMA. The effect of the radius of curvature is investigated and a thorough comparison with the corresponding flat counterparts is provided. Then, two prototypes of the symmetrical NEGCOMA have been manufactured and measured to assess the simulated results. The experimental verification is reported in Section III, showing a very good agreement between simulations and measurements. In the fourth and last Section, the conclusions of this work are drawn.

II. ANTENNA DESIGN AND SIMULATIONS

Figure 1 shows a generalized dimensional sketch of the proposed curved NEGCOMA from a 3D perspective

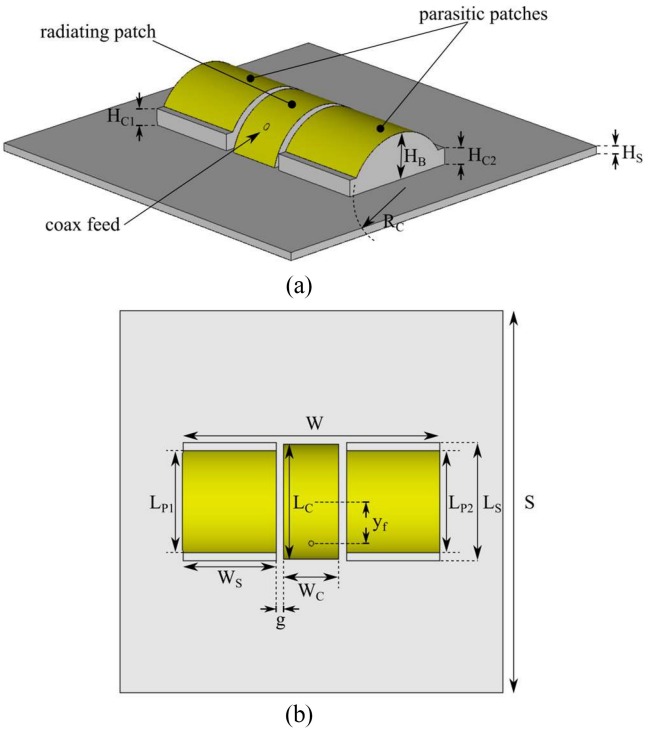

FIGURE 1. Generalized dimensional drawing of the curved NEGCOMA: a) 3D view b) top view.

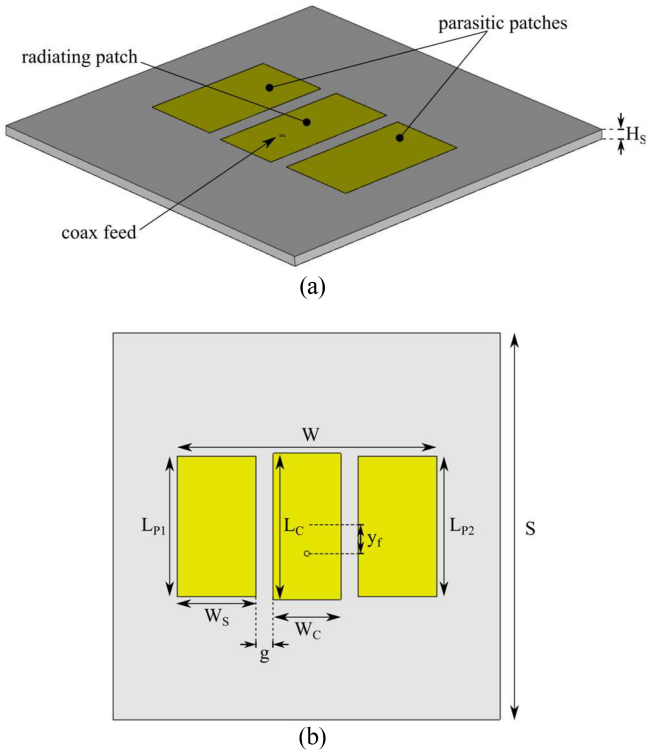

FIGURE 2. Generalized dimensional drawing of the flat NEGCOMA: a) 3D view b) top view.

(Fig. 1a) and a top view (Fig. 1b) that will be used to describe both symmetrical and asymmetrical layouts. The bottom substrate is an $S \times S$ square with thickness H_S made of Polylactic Acid (PLA) with dielectric permittivity $\varepsilon_r = 2.55$ and $\tan\delta = 0.008$ at 2.45 GHz, wherein $S = 100$ mm and $H_S = 2$ mm. The radiating and parasitic patches are supported by a cylindrical protrusion with radius R_C, made also of PLA. However, the supporting structure of the side patches is slightly different from the central one. In fact, the resonant length of the central patch is dictated solely by the height of the cylindrical protrusion H_B. On the other hand, in the lateral supporting structures, there is a small step that breaks the circular profile on both sides (as it can be clearly seen in Fig. 1a), which is useful for having an accurate sizing of the parasitic patches, since the patch metallization is provided via adhesive aluminum tape. The height of the steps is H_{C1} and H_{C2}, which are equal for the symmetrical NEGCOMA. The central patch and the side patches are characterized by a width W_C and W_S, respectively, whereas the projected planar resonant sizes of the central patch and side patches are L_C and L_{P1}, L_{P2}, respectively. The total length of the side structures is equal to L_S (see Fig. 1b) also including the width of the steps. To achieve the NEGCOMA layout, the central and side patches are separated by a gap g. Finally, the total width, accounting for central and side patches width plus the gaps, is W, which is set to 67 mm for all the configurations considered in the following.

The feeding is provided through a SMA coaxial connector, with the feeding point located at y_f with respect to the center of the antenna. The design strategy for the antenna is similar to the one described in [5], wherein the first step is the choice of the curvature radius and then the selection of a proper height H_B (which sets the resonant length L_C) to obtain the main resonance at the selected design frequency. Without loss of generality, we consider here the center frequency at 2.45 GHz, to allow a consistent comparison with the results of [5]. Then the NEGCOMA configuration is exploited, based on the same design consideration reported in [8], optimizing the length of the side patches and the gap g in order to achieve the impedance matching in the widest possible bandwidth. The widths of the center patch W_C and of the side patches W_S have been used as further design parameters, but always maintaining the total width of the antenna equal to 67 mm. Finally, the position of the coaxial feed y_f is chosen to match the 50 Ω impedance of the commercial coaxial connector.

For bandwidth comparison, curved asymmetrical, flat symmetrical, and flat asymmetrical versions of the NEGCOMA have been also designed and simulated using the same PLA substrate. The dimensional drawing of the flat NEGCOMA is reported in Fig. 2. Also in these cases the total width W has been fixed to 67 mm.

The antennas design and optimization, based on the design strategy described above, have been carried out using the commercial software CST Studio Suite.

To investigate the features of the curved NEGCOMA, a parametric analysis has been performed on the symmetrical configuration for different values of the radius of curvature R_C. The minimum value of R_C has been set to 16 mm.

TABLE 2. Geometrical parameters of the symmetrical NEGCOMA. H_S = 2 mm, W = 67 mm, S = 100 mm.

R_C (mm)	H_B (mm)	H_{C1} =H_{C2} (mm)	L_{P1} = L_{P2} (mm)	L_S (mm)	W_S (mm)	W_C (mm)	g (mm)	L_C (mm)	y_f (mm)
∞	0	0	36.25	36.25	20.25	17.5	4.5	37.75	7
40	3.12	0.5	31.15	40	21	17	4	33.25	11
30	5.53	1.25	30.8	36	21	17	4	34.6	11.5
20	8	2	28.5	34	22	15	4	31.9	10.25
16	11.8	4.2	26.7	31	24.35	14.3	2	30.14	10.87

TABLE 3. Geometrical parameters of the asymmetrical NEGCOMA. H_S = 2 mm, W = 67 mm, S = 100 mm.

R_C (mm)	H_B (mm)	H_{C1} (mm)	H_{C2} (mm)	L_{P1} (mm)	L_{P2} (mm)	L_S (mm)	W_S (mm)	W_C (mm)	g (mm)	L_C (mm)	y_f (mm)
∞	0	0	0	37.05	35.8	-	24.5	13	2.5	38.8	7
16	12.8	4	6	28.6	26.2	32	24.5	14	2	31.4	11

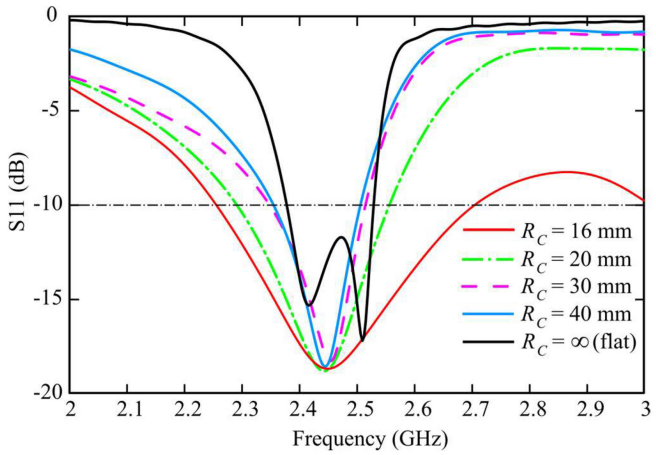

FIGURE 3. Reflection coefficient (S11) of the symmetrical NEGCOMA for selected values of the radius of curvature R_C.

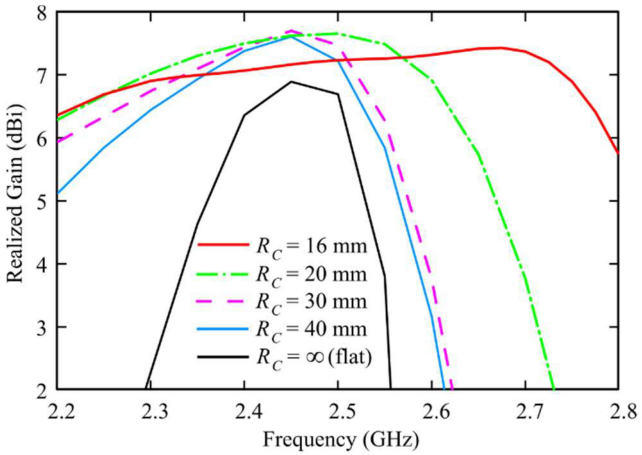

FIGURE 4. Realized gain of the symmetrical NEGCOMA for selected values of the radius of curvature R_C.

Lower values could be possible but they would increase the total antenna height ($H_B + H_S$) and have been avoided since the longer the coaxial probe, the higher the inductive contribution to the input impedance [15], which makes difficult to match the antenna. In Fig. 3, we report the simulated reflection coefficient (S11) of the symmetrical NEGCOMA for a range of selected values of the curvature radius R_C. The corresponding flat layout is displayed with a curvature radius virtually infinite. As expected, the progressive reduction in the curvature radius results in a fractional bandwidth increase, which is consistent with [5]. Specifically, the fractional bandwidth goes from 6.1% (149 MHz) of the flat NEGCOMA to 18% (440 MHz) of the curved one with R_C = 16 mm.

In Fig. 4, the realized gain for the same range of curvature radii is shown. It is pretty clear that the realized gain of the curved symmetrical NEGCOMA with R_C = 16 mm is rather stable throughout the entire operating band, ranging from 6.5 dBi to 7.3 dBi.

The complete geometrical parameters of the designed symmetrical NEGCOMAs are reported in Table 2, whereas the results reported in Figs. 3 and 4 are summarized in Table 4, where in addition to the realized gain G_R and the bandwidth B, we also report the directivity Dir, and the

TABLE 4. Simulated electromagnetic performance of the symmetrical NEGCOMA at 2.45 GHz.

R_C (mm)	G_R (dBi)	Dir (dBi)	η (%)	B (%)	B (MHz)
∞	6.89	8.13	77.7	6.10	149
40	7.60	8.20	88.5	6.16	151
30	7.70	8.26	89.7	6.77	166
20	7.62	8.05	92.5	10.81	265
16	7.16	7.44	95.6	18.00	440

radiation efficiency η. The benefits of adopting a curved configuration over a flat one for the NEGCOMA layout are undeniable. Other than a wider bandwidth, the curved configuration exhibits also a larger efficiency with respect to its flat counterpart, increasing from 77.7% to 95.6%.

Finally, in Fig. 5, the radiation pattern of the symmetrical NEGCOMA for R_C = 16 mm is reported for 2.25 GHz, 2.45 GHz, and 2.65 GHz. As expected, the far-field pattern of the symmetrical NEGCOMA maintains the maximum in the broadside direction in the whole operating band. Fig. 5 also reports the measured pattern, which will be discussed in the next section. The simulated cross-polar component in the E-plane is not shown because it is lower than −50 dB.

For the sake of completeness, the performance of the asymmetrical NEGCOMA has been investigated, though the

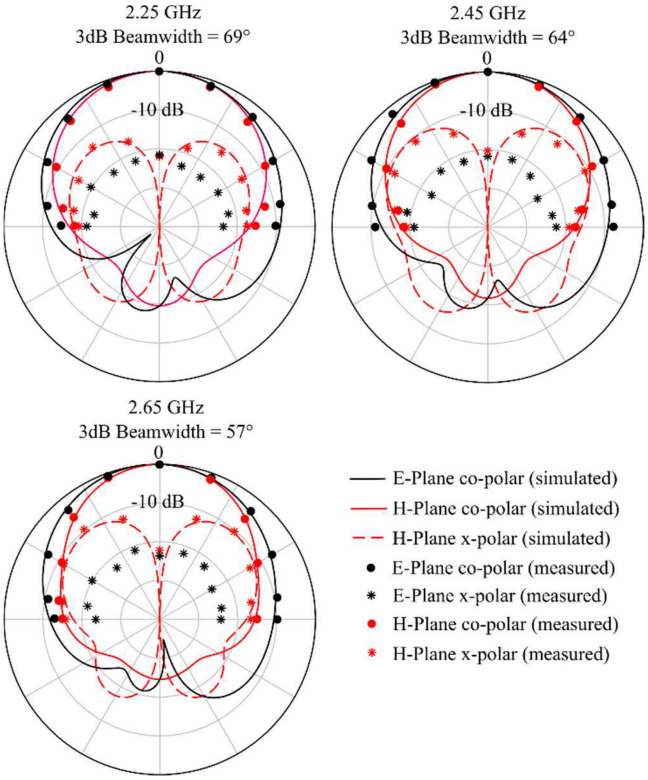

FIGURE 5. Simulated and measured far-field pattern of the symmetrical NEGCOMA for $R_c = 16$ mm.

far-field pattern of this configuration is strongly dependent on the frequency within the operating band. The geometrical parameters of the designed asymmetrical NEGCOMA are reported in Table 3, for both the curved configuration and the flat counterpart.

In Fig. 6, the simulated reflection coefficient comparison between curved and flat asymmetrical NEGCOMA is displayed. The flat layout is characterized by a fractional bandwidth of 8.2% (201 MHz) whereas the curved layout exhibits a total bandwidth of 31.5% (772 MHz), once again confirming the ability of the curved configuration to significantly enhance the operating bandwidth of planar antennas. With no surprise, the asymmetrical curved NEGCOMA outperforms the symmetrical layout, almost doubling the bandwidth. Nonetheless, the asymmetrical NEGCOMA generates sub-optimal radiation patterns, wherein the radiation maximum does not match with the broadside direction, as it can be clearly stated looking at the simulated realized gain shown in Fig. 7 as well as the simulated far-field patterns reported in Fig. 8 for selected frequencies in the operating band.

III. ANTENNA FABRICATION AND EXPERIMENTAL VERIFICATION

The dielectric substrate of the antenna has been fabricated using the commercial 3D-printer PRUSA MK3S+ and a PLA thermoplastic filament, setting a 100% infill and an aligned rectilinear pattern (with 90° cross-hatching) with

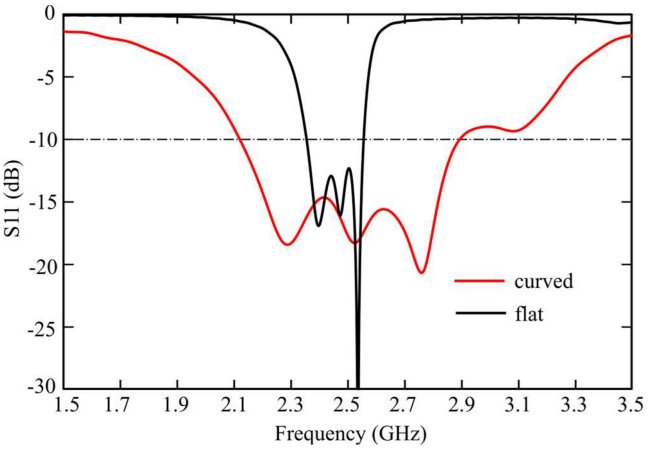

FIGURE 6. Simulated reflection coefficient (S11) of the flat and curved asymmetrical NEGCOMA with $R_c = 16$ mm.

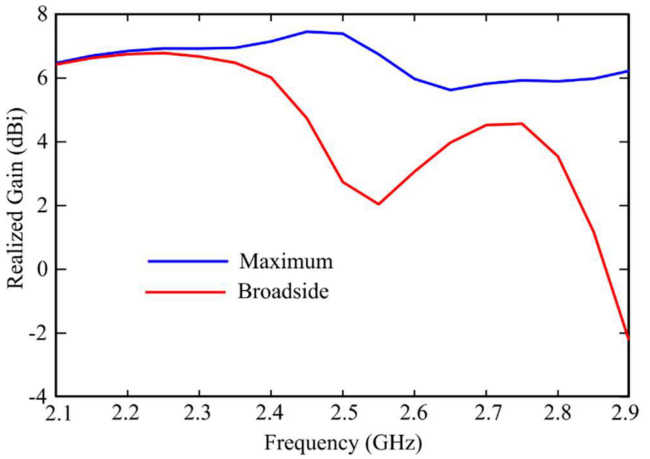

FIGURE 7. Simulated realized gain for the maximum and the broadside directions of the curved asymmetrical NEGCOMA with $R_c = 16$ mm.

0.2 mm-thick layers. The nozzle diameter is 0.4 mm and the extruding temperature is set to 210 °C.

The dielectric permittivity of the PLA has been computed using the T-resonator method [16]. The metallization of the patches and ground plane has been provided using 50μm-thick adhesive aluminum tape, manually cut to obtain the designed dimensions. The coaxial connector has been glued to the aluminum tape by using a silver-loaded conductive epoxy adhesive (see Fig. 9).

Two (virtually) identical prototypes of the curved symmetrical 3D-printed NEGCOMA designed in Section II have been manufactured (Fig. 9). Then, the electromagnetic performance has been measured in an anechoic environment (Fig. 10) by using the Anritsu MS46322B two-port vector network analyzer (VNA). The broadside realized gain of the antenna under test (AUT) has been measured by the two-antenna method (as defined in [17, Sec. 8.3]) assuming that the two manufactured prototypes are identical.

In Figs. 11 and 12, the reflection coefficient and the realized gain of the AUT are plotted, respectively. The agreement between simulated results and measurement is very

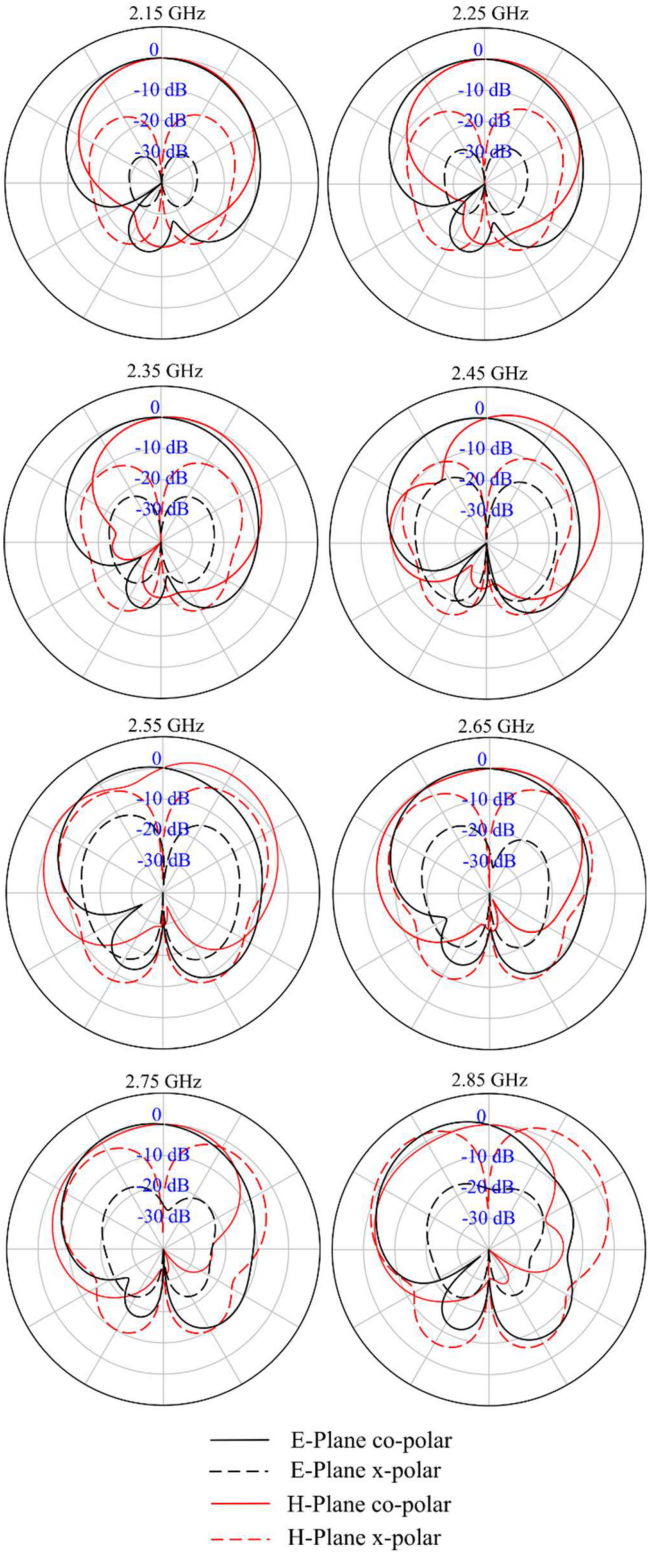

FIGURE 8. Simulated far-field pattern of the curved asymmetrical NEGCOMA with $R_C = 16$ mm.

good, with a measured bandwidth of about 400 MHz (16.3% fractional bandwidth).

Finally, the far-field pattern of the fabricated prototype in the principal cuts has been measured at three selected

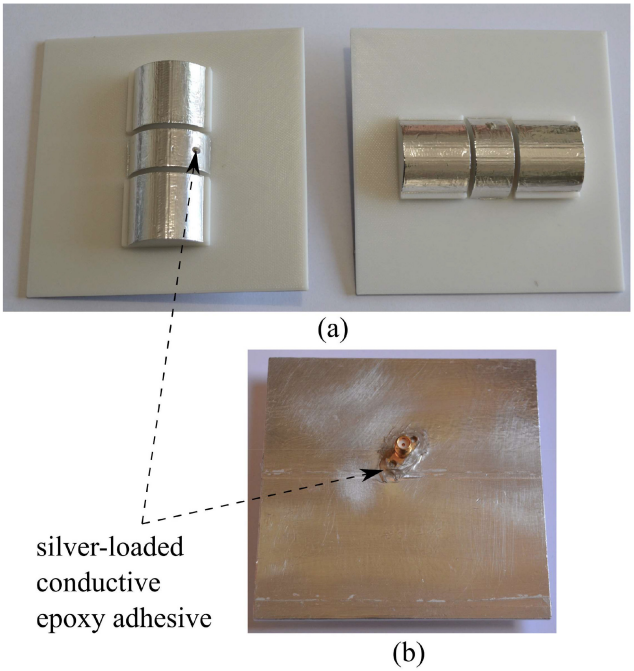

FIGURE 9. Photo of the manufactured prototypes: (a) front, (b) back.

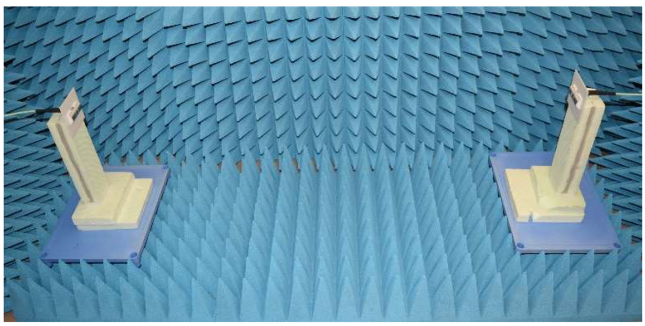

FIGURE 10. Experimental set up for the measurement of the realized gain by the two-antenna method [17].

frequencies in the operating band, i.e., 2.25 GHz, 2.45 GHz, and 2.65 GHz (see Fig. 5). The measurement setup is the same as in Fig. 10, but one of the AUTs has been placed on a rotating plate and the other one has been replaced by a test calibrated antenna (model HyperLOG 7060 by AARONIA AG), which has been connected to a broadband Low Noise Amplifier (LNA) (model ZX60-83LNS+ by Minicircuits) to improve the measurement sensitivity. A good agreement between simulation and measurement is observed. It should be noted that the back-radiation has not been measured due to the obstacle represented by the test coaxial cable connected to the VNA.

IV. CONCLUSION

The recent development of fast prototyping techniques, such as additive manufacturing 3D-printing technology, has enabled the deployment of unconventional layouts also in the antenna design. Specifically, taking advantage of the free-form factor of the 3D-printing, the substrate of patch

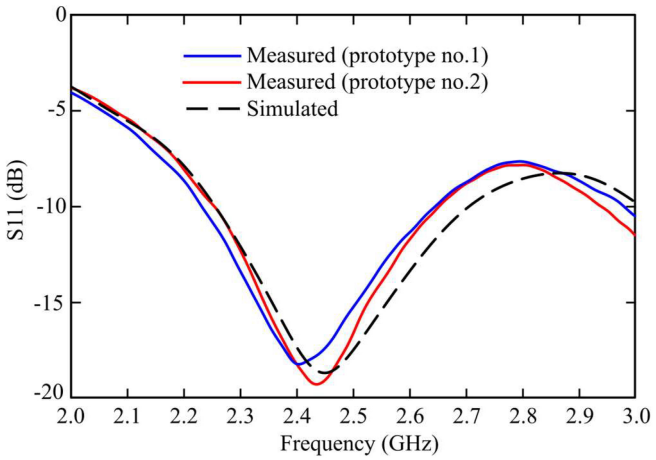

FIGURE 11. Comparison between simulated and measured reflection coefficient (S11) of the manufactured prototypes.

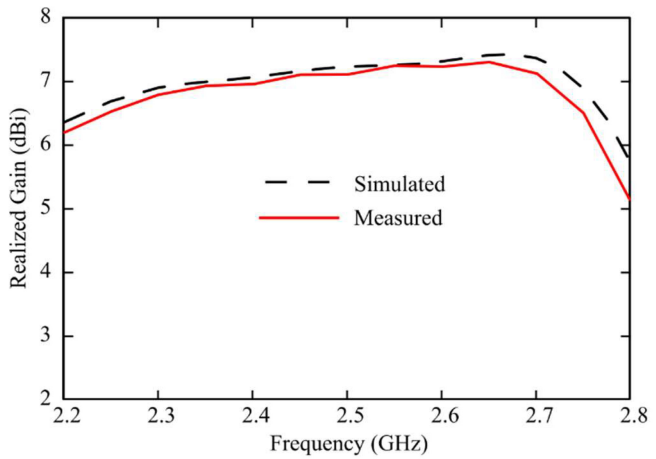

FIGURE 12. Comparison between simulated and measured broadside realized gain of the manufactured prototype.

antennas can now exploit a third dimension in order to boost the antenna performance, such as achieving wider bandwidth and higher efficiency. It has also been demonstrated that combining already existing techniques, well-known in the open literature, with the advantages offered by this new manufacturing process, can further improve the antenna performance. In this context, a novel 3D-printed curved NEGCOMA has been proposed, merging the curved layout [5] with the non-radiating edge gap-coupled configuration [8] to obtain bandwidth enhancement and planar size reduction with respect to the flat NEGCOMA. Indeed, the presented curved symmetrical NEGCOMA achieves an overall fractional bandwidth of 16.3%, against a 6.1% bandwidth of the flat NEGCOMA. The proposed configuration also improves the bandwidth of the standard curved antenna [5] that exhibits a 9% bandwidth. The analysis of the asymmetrical curved NEGCOMA has also been performed. The latter features a fractional bandwidth of 31.5%, greatly outperforming its planar counterpart. However, this configuration is flawed by a non-optimal radiation pattern, wherein the maximum gain direction is shifted from the broadside, making this layout not suitable for certain applications.

The measured results on the manufactured curved symmetrical NEGCOMA show an excellent agreement between simulation and measurement. It is worth noting that at 2.45 GHz the manufacturing tolerance of the curved profile, which is approximated by 0.2mm-thick steps, is not critical since the resolution of the commercial 3D printer used in this work is small compared to the wavelength. This aspect should be properly investigated for higher operating frequencies to establish the limitations of approximating by steps the curved profile when using 3D printing manufacturing technology. However, the proposed curved NEGCOMA can be ideally scaled at a higher and arbitrary frequency and good results are expected as long as the designer employs high-resolution printers (or other improved fabrication techniques) to realize the curved profile and he is able to provide high-precision cutting or deposition of the metal patch.

REFERENCES

[1] D. Helena, A. Ramos, T. Varum, and J. N. Matos, "Antenna design using modern additive manufacturing technology: A review," *IEEE Access*, vol. 8, pp. 177064–177083, 2020.

[2] T. Whittaker, S. Zhang, A. Powell, C. J. Stevens, J. Y. C. Vardaxoglou, and W. Whittow, "3D printing materials and techniques for antennas and metamaterials: A survey of the latest advances," *IEEE Antennas Propag. Mag.*, early access, Dec. 26, 2022, doi: 10.1109/MAP.2022.3229298.

[3] R. J. Beneck, G. Mackertich-Sengerdy, S. Soltani, S. D. Campbell, and D. H. Werner, "A shape generation method for 3D printed antennas with unintuitive geometries," *IEEE Access*, vol. 10, pp. 91294–91305, 2022.

[4] Y. Tawk and J. Costantine, "A polarization reconfigurable 3D printed dual integrated quadrifilar helix antenna array embedded within a cylindrical dielectric mesh," *IEEE Trans. Antennas Propag.*, vol. 71, no. 1, pp. 309–317, Jan. 2023.

[5] G. Muntoni et al., "A curved 3-D printed microstrip patch antenna layout for bandwidth enhancement and size reduction," *IEEE Antennas Wireless Propag. Lett.*, vol. 19, no. 7, pp. 1118–1122, Jul. 2020, doi: 10.1109/LAWP.2020.2990944.

[6] G. Montisci, G. Mura, G. Muntoni, G. A. Casula, F. P. Chietera, and M. Aburish-Hmidat, "A curved microstrip patch antenna designed from transparent conductive films," *IEEE Access*, vol. 11, pp. 839–848, 2023.

[7] G. Muntoni et al., "A curved 3D-printed S-band patch antenna for plastic CubeSat," *IEEE Open J. Antennas Propag.*, vol. 3, pp. 1351–1363, 2022.

[8] G. Kumar and K. Gupta, "Nonradiating edges and four edges gap-coupled multiple resonator broad-band microstrip antennas," *IEEE Trans. Antennas Propag.*, vol. 33, no. 2, pp. 173–178, Feb. 1985.

[9] M. El Hammoumi et al., "A wideband 5G CubeSat patch antenna," *IEEE J. Miniat. Air Space Syst.*, vol. 3, no. 2, pp. 47–52, Jun. 2022.

[10] J. Kornprobst, K. Wang, G. Hamberger, and T. F. Eibert, "A mm-Wave patch antenna with broad bandwidth and a wide angular range," *IEEE Trans. Antennas Propag.*, vol. 65, no. 8, pp. 4293–4298, Aug. 2017.

[11] M. Xue, W. Wan, Q. Wang, and L. Cao, "Low-profile wideband millimeter-wave antenna-in-package suitable for embedded organic substrate package," *IEEE Trans. Antennas Propag.*, vol. 69, no. 8, pp. 4401–4411, Aug. 2021.

[12] H. H. Tran and N. Nguyen-Trong, "Performance enhancement of MIMO patch antenna using parasitic elements," *IEEE Access*, vol. 9, pp. 30011–30016, 2021.

[13] J.-F. Qian, F.-C. Chen, Q.-X. Chu, Q. Xue, and M. J. Lancaster, "A novel electric and magnetic gap-coupled broadband patch antenna with improved selectivity and its application in MIMO system," *IEEE Trans. Antennas Propag.*, vol. 66, no. 10, pp. 5625–5629, Oct. 2018.
[14] J. Singh, R. Stephan, and M. A. Hein, "Low-profile Penta-band automotive patch antenna using horizontal stacking and corner feeding," *IEEE Access*, vol. 7, pp. 74198–74205, 2019.
[15] P. S. Hall, "Probe compensation in thick microstrip patches," *Electron. Lett.*, vol. 23, no. 11, pp. 606–607, May 1987.
[16] R. Colella et al., "Electromagnetic characterisation of conductive 3D-printable filaments for designing fully 3D-printed antennas," *IET Microw., Antennas Propag.*, vol. 16, no. 11, pp. 687–698, Sep. 2022.
[17] *IEEE Recommended Practice for Antenna Measurements*, IEEE Standard 149, 2021.

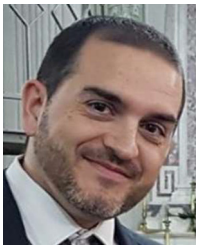

GIACOMO MUNTONI received the bachelor's degree in electronic engineering, the master's degree in telecommunication engineering, and the Ph.D. degree in electronic engineering and computer science from the University of Cagliari in 2010, 2015, and 2019, respectively.

He is currently working as a Technologist with the Applied Electromagnetics Group, University of Cagliari. His research activity involves design and characterization of antennas for biomedical and aerospace applications, microwave–based dielectric characterization of materials, 3-D printing of RF components, and monitoring of the space debris environment in low-Earth orbit with the Sardinia Radio Telescope, in collaboration with Cagliari Astronomical Observatory.

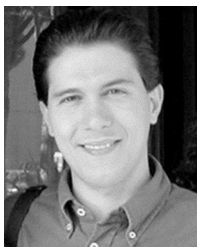

GIOVANNI A. CASULA (Senior Member, IEEE) received the M.S. degree in electronic engineering and the Ph.D. degree in electronic engineering and computer science from the University of Cagliari, Cagliari, Italy, in 2000 and 2004, respectively.

Since December 2017, he has been an Associate Professor of Electromagnetic Fields with the University of Cagliari, teaching courses in electromagnetics and antenna engineering. He has authored or coauthored about 50 papers in international journals. His current research interests include the analysis and design of waveguide slot arrays, RFID antennas, wearable antennas, numerical methods in electromagnetics. He is an Associate Editor of IEEE TRANSACTIONS ON ANTENNAS AND PROPAGATION, IET MICROWAVES, ANTENNAS & PROPAGATION, *Electronics* (MDPI), and Sensors (MDPI) and an Academic Editor of the *International Journal of Antennas and Propagation*.

GIORGIO MONTISCI (Senior Member, IEEE) received the M.S. degree in electronic engineering and the Ph.D. degree in electronic engineering and computer science from the University of Cagliari, Cagliari, Italy, in 1997 and 2000, respectively. Since February 2022, he has been a Full Professor of Electromagnetic Fields with the University of Cagliari, teaching courses in electromagnetics and microwave engineering. He has authored or coauthored 80 papers in international journals. His current research interests include the analysis and design of waveguide slot arrays, RFID antennas, wearable antennas, numerical methods in electromagnetics, and microwave circuits and systems. He was awarded the IEEE Access outstanding Associate Editor of 2020 and 2021. He is an Associate Editor of IEEE ACCESS, *IET Microwaves, Antennas & Propagation*, and *IET Electronics Letters* and an Academic Editor of the *International Journal of Antennas and Propagation*.

Open Access funding provided by 'Università degli Studi di Cagliari' within the CRUI CARE Agreement